W.P. LV, W. LI

ISSN 0543-5846
METABK 63(2) 261-263 (2024)
UDC – UDK 621.771:621.833.831:531.3:658.511=111

DYNAMIC CHARACTERISTICS ANALYSIS OF ROLLING MILL GEAR REDUCER USING NUTATION FACE GEAR TRANSMISSION

Received – Primljeno: 2023-10-11
Accepted – Prihvaćeno: 2023-12-20
Original Scientific Paper – Izvorni znanstveni rad

The nutation face gear transmission system has advantages such as high reduction ratio, high power density, compact structure, and smooth transmission, making it suitable for high-power transmission in metallurgical machinery, tunnel boring machines, and other applications. In this study, a 12-degree-of-freedom bending-torsion-axial coupling dynamic model of the transmission system is established. The impact of mesh stiffness amplitude on the dynamic characteristics of the novel rolling mill gear reducer is considered. The research indicates that an increase in gear pair mesh stiffness leads to an increase in torsional vibration amplitude.

Keywords: rolling mill, gear, dynamic characteristics, analysis, transmission

INTRODUCTION

As one of the key production equipment in the metallurgical industry, the performance of gear reducers in rolling mills operating at low speed and heavy load significantly affects the stability and efficiency of the entire system [1-3]. The traditional gear transmission part of the rolling mill transmission system often uses helical gears, which may result in substantial alternating torque and impact vibration during the rolling process, causing fatigue damage and harm to system components [4-5]. The adoption of face gears instead of helical gears is expected to effectively improve the instability of torsional direction transmission [6]. This study provides a reference basis for the design and engineering application of low-speed, high-torque rolling mill gear reducers.Figure 1 shows a schematic diagram of the nutation face gear transmission structure.

SYSTEM DYNAMICS MODEL

For convenient dynamic modeling of the nutation face gear transmission system, without loss of generality, the following assumptions are made:

1) Friction on gear surfaces during meshing is neglected;
2) System damping is considered as general viscous damping.

A bending-torsion-axial coupling analysis model of the nutation face gear transmission system is established using the lumped parameter method, as shown in Figure 2.

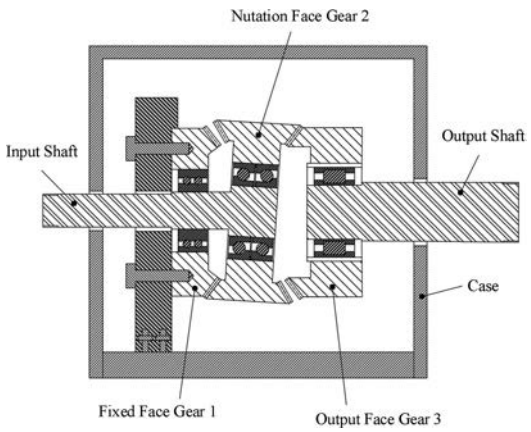

Figure 1 Schematic diagram of nutation face gear transmission system

In the Figure 2, k_{pi}, c_{pi} (p=x, y, z; i=1,2,3) represent the bearing stiffness and support damping received by each gear in the three coordinate directions. k_{u1}, c_{u1} represent the torsional stiffness and torsional damping of the fixed face gear about the z-axis. km_j, cm_j, and e_j (j=1,2) represent the time-varying mesh stiffness, mesh damping, and mesh error for each gear pair respectively. T_{in} represents the input torque on the nutation face gear, and T_{out} represents the load torque on the output face gear. the global coordinate system of the system is denoted as O-xyz, satisfying the right-hand rule. Local coordinate systems, denoted as O_i-$x_i y_i z_i$, are established at concentrated mass points on each face gear, also satisfying the right-hand rule. The directions of the local coordinate systems for each face gear are the same as the global coordinate system. The variables x_i, y_i, z_i, and θ_i are defined as the translational vibration displacement and torsional vibration line displacement about the z-axis for each face gear in the x, y, z directions.

W.P. Lv, W. Li (E-mail: lw201906@ncst.edu.cn), College of Mechanical Engineering, North China University of Science and Technology, Hebei, Tangshan, China.

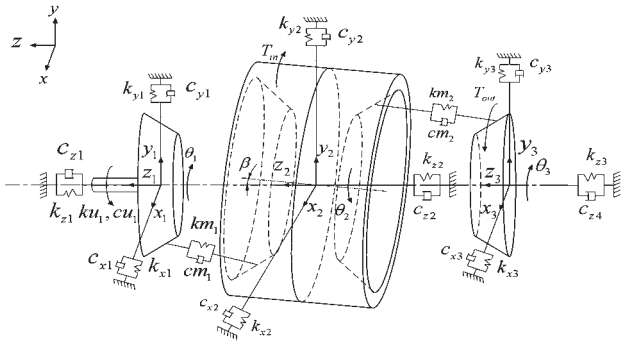

Figure 2 Dynamic model of the nutation face gear transmission system

Derivation of motion differential equations

This system has a total of 12 degrees of freedom, with generalized coordinates as follows:

$$Q = \{x_1, y_1, z_1, \theta_1, x_2, y_2, z_2, \theta_2, x_3, y_3, z_3, \theta_3\}^T \quad (1)$$

Under the action of meshing force, taking compression along the meshing line as positive, the normal displacement U_1 of the fixed face gear 1 can be expressed as:

$$\begin{cases} u_1 = \cos(\alpha_1)(x_1 - x_2) + \sin(\alpha_1)\cos(\delta_1)(y_2 - y_1) + \\ \sin(\alpha_1)\sin(\delta_1)(z_2 - z_1) + \cos(\alpha_1)(\theta_2 r_2 + \theta_1 r_1) \\ u_2 = \cos(\alpha_3)(x_2 - x_3) + \sin(\alpha_3)\cos(\delta_3)(y_3 - y_2) + \\ \sin(\alpha_3)\sin(\delta_3)(z_3 - z_2) + \cos(\alpha_3)(\theta_2 r_2 + \theta_3 r_3) \end{cases} \quad (2)$$

Here, α represents the pressure angle of face gear, and δ represents the cone angle of face gear.

According to the analysis of meshing line displacement above, the dynamic meshing force between gear pairs can be obtained as:

$$\begin{cases} F_{m1} = c_{m1}\dot{u}_1 + k_{m1}u_1 \\ F_{m2} = c_{m2}\dot{u}_2 + k_{m2}u_2 \end{cases} \quad (3)$$

Considering factors such as time-varying mesh stiffness, meshing damping, gear tooth errors, etc., according to Newton's second law, the following motion differential equations can be derived.

Fixed face gear 1:

$$\begin{cases} m_1\ddot{x}_1 + \cos(\alpha_1)F_{m1} + k_{x1}x_1 + c_{x1}\dot{x}_1 = 0 \\ m_1\ddot{y}_1 - \sin(\alpha_1)\cos(\delta_1)F_{m1} + k_{y1}y1 + c_{y1}\dot{y}_1 = 0 \\ m_1\ddot{z}_1 - \sin(\alpha_1)*\sin(\delta_1)*F_{m1} + k_{z1}*z_1 + c_{z1}*\dot{z}_1 = 0 \\ I_1\ddot{\theta}_1 + \cos(\alpha_1)*F_{m1}*r_1 + k_{u1}*\theta_1 + c_{u1}*\dot{\theta}_1 = 0 \end{cases} \quad (4)$$

Nutation face gear 2:

$$\begin{cases} m_2\ddot{x}_2 - \cos(\alpha_1)*F_{m1} + \cos(\alpha_3)*F_{m2} + k_{x2}*x_2 \\ + c_{x2}\dot{x}_2 = 0 \\ m_2\ddot{y}_2 + \sin(\alpha_1)*\cos(\delta_1)*F_{m1} - \sin(\alpha_3)*\cos(\delta_3)*F_{m2} \\ + k_{y_2}*y_2 + c_{y2}\dot{y}_2 = 0 \\ m_2\ddot{z}_2 + \sin(\alpha_1)*\sin(\delta_1)*F_{m1} - \sin(\alpha_3)*\sin(\delta_3)*F_{m2} \\ + k_{z2}*z_2 + c_{z2}\dot{z}_2 = 0 \\ I_2\ddot{\theta}_2 + \cos(\alpha_1)*F_{m1}*r_2 + \cos(\delta_3)*F_{m2}*r_2 = 0 \end{cases} \quad (5)$$

Rotating face gear 3:

$$\begin{cases} m_3\ddot{x}_3 - F_{m2}*\cos(\alpha_3) + k_{x3}*x_3 \\ + c_{x3}*\dot{x}_3 = 0 \\ m_3\ddot{y}_3 + F_{m2}*\sin(\alpha_3)*\cos(\delta_3) \\ + k_{y3}*y_3 + c_{y3}*\dot{y}_3 = 0 \\ m_3\ddot{z}_3 + F_{m2}*\sin(\alpha_3)*\sin(\delta_3) \\ + k_{z3}*z_3 + c_{z3}*\dot{z}_3 = 0 \\ I_3\ddot{\theta}_3 + F_{m2}*\cos(\alpha_3)*r_3 = -T_{out} \end{cases} \quad (6)$$

To avoid the phenomenon of ill-conditioned results in the solving process of the differential equations due to significant differences in parameter magnitudes, it is necessary to normalize them. Due to space limitations, the dimensionless form of the differential equations after normalization is not presented here. The normalized differential equations are solved using a 4th-order Runge-Kutta method to obtain parameters such as displacement, velocity, and acceleration. Subsequently, an analysis of the dynamic response of the oscillating face gear transmission system is conducted.

DYNAMIC CHARACTERISTICS ANALYSIS

Gear parameters refer to literature [7], and an input speed of 700 rpm is chosen, with torsional vibration displacement of the nutation face gear as the main indicator to investigate the system's vibration degree.

To study the influence of mesh stiffness on system vibration, five different multiples of average mesh stiffness (0,5 times, 0,75 times, 1 time, 1,25 times, 1,5 times) are taken as system excitations (with other factors constant). The variation pattern of torsional vibration displacement with dimensionless time under different multiples of average mesh stiffness is shown in Figure 3.

From the Figure 3, it is observed that the larger the mesh stiffness, the greater the gear vibration amplitude, with an increment around 20 μm. Mesh stiffness significantly affects the system's vibration characteristics.

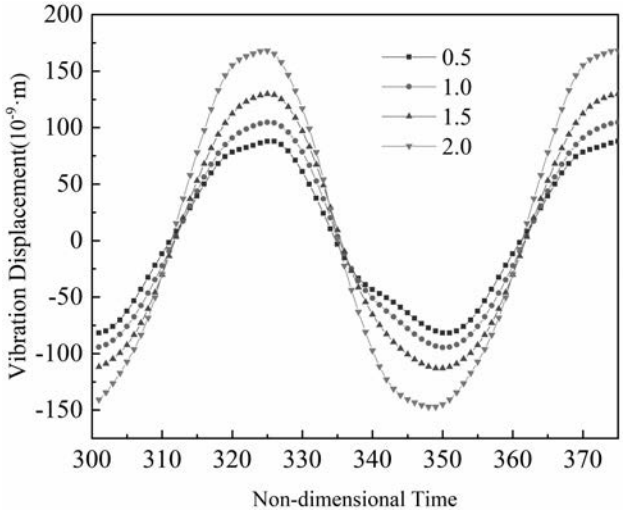

Figure 3 The variation pattern of torsional vibration displacement with dimensionless time under different multiples of average mesh stiffness.

To investigate the impact of gear support stiffness on system vibration, taking the radial supporting stiffness k_{y3} of the output gear 3 as an example, five different multiples of supporting mesh stiffness (0.5 times, 1 times, 1.5 times, 2 times) were selected as the system excitation with other factors held constant. The variation pattern of torsional vibration displacement with dimensionless time under different radial support stiffness conditions is shown in Figure 4.

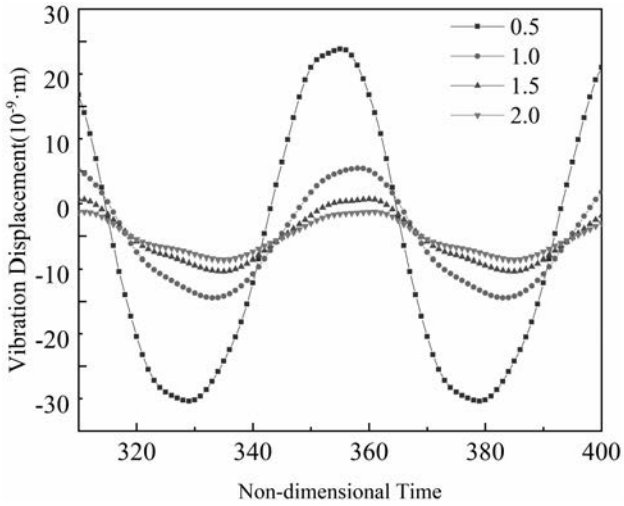

Figure 4 The variation pattern of torsional vibration displacement with dimensionless time under different multiples of support stiffness.

From the Figure 4, it can be observed that as the support stiffness increases, the gear vibration amplitude decreases, and the amplitude is around 10 μm. Increasing the radial support stiffness of the output gear 3 effectively reduces system vibration.

To study the influence of input speed on system vibration, five different input speeds (500 rpm, 700 rpm, 900 rpm, 1000 rpm) were considered, while keeping other factors constant. The variation pattern of torsional vibration displacement with dimensionless time under different multiples of average mesh stiffness is shown in Figure 5.

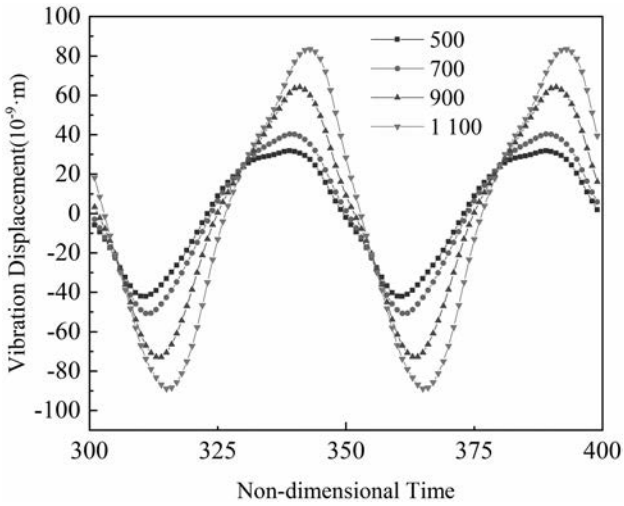

Figure 5 The variation pattern of torsional vibration displacement with dimensionless time under different multiples of input speed.

From the Figure 5, it is evident that higher input speeds lead to larger gear vibration amplitudes, with amplitudes around 15 μm. Properly reducing the input speed can effectively improve the system's vibration.

CONCLUSION

From the above analysis, it can be concluded that input speed, mesh stiffness, and support stiffness have a significant impact on the torsional vibration of gears,and the impact of mesh stiffness is most pronounced.. Reducing the mesh stiffness of the gear pair, increasing the radial support stiffness of the output gear 3, and appropriately decreasing the input speed can effectively control the amplitude of torsional vibration in each gear, thereby reducing the overall system vibration. This analysis holds great promise for application in rolling mill reducers.

ACKNOWLEDGMT

This work was supported in part by the "Tangshan Science and Technology Plan Project" of Tangshan City under Grant 21130216C and 22130209G.

REFERENCES

[1] Rednikov N S, N S R, N E A, et al. Integrated Diagnostic Method Analysis of Use in the Inspection of Rolling Mills[J]. IOP Conference Series: Materials Science and Engineering,2020,969(1).

[2] R.Du, Z.Q.Liu, L.Ge, et al. A New Electrohydraulic Hybrid Energy-Saving System Used on the Reversible Rolling Mills[J]. Advances in Materials Science and Engineering,2023.

[3] W. N N,B. H R. Condition monitoring and fault detection in roller bearing used in rolling mill by acoustic emission and vibration analysis[J]. Materials Today: Proceedings, 2022.

[4] Z Wang, P.Ning, X.Pan, et al. Analysis of the Causes of Failure and Countermeasures for Rolling Mill Reducer Roller Bearings[J]. Journal of Qiqihar University (Natural Science Edition), 2021, 37(05): 38-43.

[5] Jiang J, Liu S, Liu B, et al. Study on vibration characteristics of rolling mill based on vibration absorber[J]. Mathematical Models in Engineering, 2019,5(2).

[6] X.D.Jia, S.W, X.Q.Y, et al. Research on Dynamic Response of Cold Rolling Mill with Dynamic Stiffness Compensation[J]. Electronics, 2023,12(3).

[7] G. Wang, L. Zhu, P. Wang and J. Deng. Meshing and Bearing Analysis of Nutation Drive with Face Gear, Recent Patents on Mechanical Engineering, 13(4)(2020) 352-365.

Note: The responsible translator for English language is W.P. Lv – NCST.